ELSEVIER

Brain Research 951 (2002) 243–254

BRAIN RESEARCH

www.elsevier.com/locate/bres

Research report

A new dynamic in vitro model for the multidimensional study of astrocyte–endothelial cell interactions at the blood–brain barrier

Luca Cucullo[a], Mark S. McAllister[a], Kelly Kight[a], Ljiljana Krizanac-Bengez[a], Matteo Marroni[a], Marc R. Mayberg[a], Kathe A. Stanness[c], Damir Janigro[a,b,*]

[a]*Department of Neurological Surgery, Cerebrovascular Research Center, Cleveland Clinic Foundation, NB20, 9500 Euclid Avenue/NB20, Cleveland, OH 44195, USA*

[b]*Department of Cell Biology, Cerebrovascular Research Center, Cleveland Clinic Foundation, Cleveland, OH 44195, USA*

[c]*Department of Neurological Surgery, University of Washington, Seattle, WA 98104, USA*

Accepted 27 June 2002

Abstract

Blood–brain barrier endothelial cells are characterized by the presence of tight intercellular junctions, the absence of fenestrations, and a paucity of pinocytotic vesicles. The in vitro study of the BBB has progressed rapidly over the past several years as new cell culture techniques and improved technologies to monitor BBB function became available. Studies carried out on viable in vitro models are set to accelerate the design of drugs that selectively and aggressively can target the CNS. Several systems in vitro attempt to reproduce the physical and biochemical behavior of intact BBB, but most fail to reproduce the three-dimensional nature of the in vivo barrier and do not allow concomitant exposure of endothelial cells to abluminal (glia) and lumenal (flow) influences. For this purpose, we have developed a new dynamic in vitro BBB model (NDIV-BBB) designed to allow for extensive pharmacological, morphological and physiological studies. Bovine aortic endothelial cells (BAEC) developed robust growth and differentiation when co-cultured alone. In the presence of glial cells, BAEC developed elevated Trans-Endothelial Electrical Resistance (TEER). Excision of individual capillaries proportionally decreased TEER; the remaining bundles were populated with healthy cells. Flow played an essential role in EC differentiation by decreasing cell division. In conclusion, this new dynamic model of the BBB allows for longitudinal studies of the effects of flow and co-culture in a controlled and fully recyclable environment that also permits visual inspection of the abluminal compartment and manipulation of individual capillaries.

Theme: Cellular and molecular biology

Topic: Blood–brain barrier

Keywords: Drug delivery; Gene therapy; Cerebral blood flow; Shear stress; Glia–vascular interaction

1. Introduction

The blood–brain barrier (BBB) maintains the homeostasis of the brain microenvironment, which is crucial for neuronal activity and function. Brain microvascular endothelial cells (EC) that constitute the blood–brain barrier are responsible for the transport of metabolites, precursors and nutrients from the blood to the brain. It is well known now that at least two key factors must be present in order for endothelial cells of either central or peripheral origin to express a barrier phenotype in vitro, which distinguish them from their peripheral counterparts: intraluminal shear stress and abluminal cellular differentiation factors [22,25,32,37,17,16]. The exposure of the apical membrane to shear stress is vital to promote growth inhibition and differentiation of endothelial cells and it also serves to induce metabolic changes which limit the oxygen and substrate consumption of such cells and allow for trafficking of metabolic fuels to the brain [16,7,31]. The second vital factor for blood–brain barrier formation by endothelial cells is exposure of these cells to not yet identified

*Corresponding author. Tel.: +1-216-445-0561; fax: +1-216-444-1466.

E-mail address: janigrd@ccf.org (D. Janigro).

0006-8993/02/$ – see front matter
PII: S0006-8993(02)03167-0

'permissive' or 'promoting' factors presumably secreted by astrocytes (e.g. α-2-macroglobulin; [13]).

The goal of any in vitro study of blood–brain barrier physiology or biology is to reproduce as many aspects as possible of the in vivo endothelial cells: expression of tight junctions between endothelial cells and the negligible permeation to sucrose or electric current flow [33]; selective and asymmetric permeability to physiologically relevant ions, such as Na^+ and K^+ [12,38]; selective permeability to molecules, based on their oil/water partition coefficient and molecular weight [2]; functional expression of mechanism of active extrusion (e.g. multi-drug resistance proteins [35]) or active transport (e.g. GLUT1 [25,41]).

A first attempt to achieve this result came from the use of bi-dimensional co-culture models [4,10,18]. Various levels of success have been achieved by use of these models, including relatively high TEER (Trans-Endothelial Electrical Resistance), expression of P-glycoprotein (PgP), etc. Recent molecular evidence suggesting that cerebral blood flow may have a unique differentiating effect on endothelial cells [11,9,19] has prompted the development of new, flow-based co-culture systems [25,7,38,30,36,27]. We developed an in vitro model of the BBB characterized by a three-dimensional, hollow fiber structure that enables co-culturing of EC with glia with endothelial cells exposed to shear stress [25,7,38,18,30,36,27,29].

In the hollow fiber apparatus, endothelial cells develop a morphology that closely resembles the endothelial phenotype in situ [27] demonstrating that endothelial cells grown with flow develop greater differentiation than after conventional culture. More recently, we reported the induction of BBB properties in endothelial cells grown in hollow fibers in the presence of extraluminally seeded glia; this induction of a BBB-specific phenotype included low permeability to intraluminal potassium, negligible extravasation of proteins, and the expression of a glucose transporter. In addition, culturing of EC with glia affected the overall morphology of the cells and induced the expression of BBB-specific ion channels [25,37,23].

The aim of the present work was to address some of the weaknesses of existing three-dimensional tissue culture apparati and develop a new generation of dynamic in vitro culture systems based on the initial design pioneered by Ballermann, Janigro and colleagues [22,17,16,7,38,18,36,27,21,34,39,40]. In particular, we wanted to: (1) Allow easy visualization of living cells; (2) Allow re-utilization of the device for many successful uses; (3) Modify the three-dimensional properties of the system to allow simultaneous modular co-culture of many easily accessible tissue culture apparati; (4) Allow for experimental manipulations of the number of hollow fibers used during individual experiments; and (5) Create a system to closely mimic the hemodynamic conditions present in pre- and post-capillaries in vivo. We used a cell combination (C6 glioma and bovine aortic endothelial cells, BAEC) that has been previously shown to replicate most of the features of the blood–brain barrier relevant to our studies [37,38,30,39].

2. Methods

2.1. Hollow fiber apparatus

Bovine Aortic Endothelial Cells (BAEC) were obtained from Dr Sage's laboratory at the University of Washington and grown in the astrocyte medium described below. C6 (a rat glial tumor line) was purchased from ATCC (Rockville, MD, USA) and grown under the same conditions. Cells were co-cultured using hollow fiber tubes (the 'capillary vessels') inside a sealed chamber (the 'extraluminal space') accessible by ports. The cartridge/hollow fiber culturing system consists of a rectangular polycarbonate hollow chamber enclosed by a permanent glass bottom and a removable polished acrylic top; a silicon gasket between the housing and the top cover provide a watertight extracapillary space. A replaceable bundle of 12 microporous polypropylene hollow fibers coated with ProNectin™ F (Protein Polymer Technologies, Inc.) is suspended in each adapter using medical grade epoxy adhesive (Epo-Tek 301) and is in continuity with gas permeable tubing to a reservoir of growth medium allowing exchange of O_2 and CO_2. A servo-controlled variable-speed pulsatile pump generates flow from the medium source through the capillary bundle allowing diffusion of nutrients out to the extra luminal space (ECS) through the 0.64 μM trans-capillary pores at a controllable rate and metabolic products are similarly removed from the cartridge. The pumping mechanism is capable of generating flow levels of 1–50 ml/min. The entire apparatus resided in a water-jacketed incubator with 5% CO_2 and could be sterilely sampled by moving it inside a laminar flow hood.

BAEC (passage 6) were seeded intraluminally and TEER was monitored for several days before C6 (passage 7) were introduced into the ECS surrounding the capillaries. The equipment used is described elsewhere [38]. EC were grown to confluence in 75 cm^2 flasks, removed with trypsin and resuspended in DMEM containing 10% Fetal Bovine Serum (FBS) and 1% PSF (Pentomycin–Streptomicin–Fungizone) in culture medium. Amounts seeded ranged from 1.5×10^6 to 2×10^6 for each loading. Flow rate was initially adjusted to 2 ml/min then increased to 4 ml/min according to the experimental requirements.

2.2. Cell metabolism: production of lactate and consumption of glucose

In conjunction with TEER monitoring, as EC cells are not microscopically visible inside the luminal portion of the cartridge, indicators of cell metabolism were used to monitor cell expansion. Depletion of the main carbohydrate component of the growth medium (glucose) and

accumulation of metabolically produced lactic acid are used as indicators of cell growth [22,25,38,39]. For this purpose luminal and extracapillary space were sampled at daily intervals. The calculations for glucose consumption (mg/day) and lactate production rates (mg/day) are based on medium replacement, volume of non-replaced medium and previous values. Glucose consumption rate (mg/day) was calculated based on the concentration of glucose in fresh and unreplaced medium in the system, according to the following equation:

$$\frac{(V_n \times G_n) + (V_o \times G_p) - (V_{total} \times G_c)}{T_c - T_p} \quad (1)$$

where V represents added volumes of medium (ml), G is the glucose concentration (mg/dl), T is time of sampling (in fractions of days; c and p indicate the immediate and previous samples, respectively), n represents fresh medium added after previous sampling, while o represents old, unreplaced medium. Lactate production rate (mg/day) was calculated similarly:

$$\frac{(V_t \times L_c) - (V_n \times L_n) + (V_u \times L_p)}{T_c - T_p} \quad (2)$$

where L refers to the concentration of lactic acid in mg/ml. A dual-channel immobilized oxidase enzyme biochemistry (YSI 2300 STAT plus glucose and lactate analyzer, YSI Inc., Yellow Springs, OH, USA) was used to measure lactate and glucose in the cell culture medium.

2.3. Hollow fiber morphology

Under sterile conditions, the cartridge was removed from the pump apparatus, the stop cocks closed, and the top cover removed. With the use of a sterile dissecting forceps with a very fine point and ultra fine scissors, two capillaries were explanted from the hollow fiber bundle in the cartridge and the terminal stubs of these capillaries were surgically saturated with the use of a polypropylene suture monofilament (Prolene 8557H from ETHICON). Capillaries taken from the cartridges were placed in 10% formalin overnight and then placed into a 30% sucrose solution. Capillaries were embedded with O.C.T. compound (Tissue-Tek 4583) and cut with a cryostat at 20 μM thickness. The capillaries were then mounted onto slides with Vectashield mounting medium with DAPI (Vector Laboratories, Burlingame, CA, USA) and visualized with fluorescent microscopy. Other samples were processed for cresyl violet staining.

2.4. Pressure analysis

A variable-speed pulsatile pump generates flow from the medium source through the capillary bundle and back to the main reservoir (for details see vendor's site at http://www.spectrapor.com/cell/index.html). The pump apparatus consists of a central eccentric camshaft that extends and retracts four separate sets of stainless steel pins in a piston-like fashion. The pins were positioned to compress a sturdy portion of the flow path in a rhythmical fashion to generate pulsatile flow. One-way valves positioned on either side of the 'pump' ensure unidirectional flow. Through the use of different pin lengths and pump speed settings, the pumping mechanism is capable of generating flow levels of 1–50 ml/min. An invasive medical blood pressure monitoring device was used to measure and record the waveform generated by the pulsatile flow. A pressure sensor was attached to the *in*tra*l*uminal *s*ampling port (ILS port) positioned at pre- and post-capillary level. After a fixed period of time of 2 min necessary to stabilize the pressure fluctuation, the pulsatile flow patterns were measured and recorded for 6 s.

2.5. Materials used for hollow fibers

Hollow fibers were purchased from Membrana (Germany). The fiber wall itself was 200±45 μm and the inner diameter of each fiber 600±90 μm giving a total diameter of each fiber of 1 mm. Twelve hollow fibers per model are usually employed and once secured, they are cut to a length of 8.6 cm. The functional length of the fiber bundle, i.e. the length exposed to extraluminal influences, was 4.2 cm. The fibers themselves are porous with a maximum pore size of 0.64 μm, as calculated by the bubble point technique and the retention of the bacterium *P. diminuta*. The single fiber total volume is 0.024 ml giving a total luminal volume of 0.288 ml. The calculated luminal surface area of a single fiber 8.6 cm in length is 1.621 cm^2 with a resultant 19.452 cm^2 luminal surface area for endothelial cell seeding. The functional external surface area of a single fiber is 1.319 cm^2, which amounts to 15.828 cm^2 available for astrocyte interaction with luminally-seeded endothelial cells. Properties were provided by the manufacturer.

Polypropylene in and of itself is a poor substrate for cellular attachment and thus requires application of a suitable matrix molecule prior to using it for successful cell culture. We have used the whole fibronectin molecule available from Sigma for coating of the fiber surfaces prior to cell inoculation. We used a final concentration of 30 μg/ml of fibronectin diluted in 1.5 ml of PBS in order to precoat the fiber surface. Once the fibers are secured in the hollow chamber, the entire unit is sterilized with ethylene oxide, the fibers were then flushed with ethanol, rinsed, and then coated with the sterile matrix preparation prior to use in experiments.

3. Results

For the experiments presented here, a total of 15 NDIV-BBB were assembled and used. The new DIV-BBB model consists of an acrylic hollow chamber enclosed by a permanent Plexiglas bottom and a removable polished top.

Fig. 1 shows a comparison of the traditional DIV-BBB model with the new in vitro model of the blood–brain barrier. Fig. 1A depicts the schematics of the apparatus. Both the DIV-BBB and the NDIV-BBB are intra-luminally perfused as indicated in *yellow*, while oxygenation and CO_2 exchange are granted by a pump mechanism. The pumping frequency, pulsatility, and velocity can be regulated electronically. Fig. 1B,C shows a diagrammatic comparison between the two models. Note that the old DIV-BBB model is circular/pentagonal, making it difficult to accommodate this capillary/Plexiglas encasement on flat surfaces such as the stage of a microscope. The design of the new DIV-BBB (C) is intentionally flat. Both the bottom and top of the cartridge can be laid on even surfaces permitting both positioning on a microscope stage as well as the stacking of many cartridges atop each other. In both figures, the dark bundles represent hollow fibers.

One of the important differences between the old DIV-BBB model and the new design consists of the fact that the NDIV-BBB can be assembled by the experimenter and that its own components can be recycled providing the appropriate sterilization steps are taken. Thus, in the NDIV-BBB, all the assembly components can be easily disassembled, including the hollow fibers, and seeded with cells, used for extensive periods of time, and then recycled by removing old fibers and replacing them with fresh hollow fibers. This is illustrated in Fig. 3. In contrast, the commercial DIV-BBB is available only as a pre-glued and assembled unit. The assembly process of one of the subculture cartridges is depicted in Fig. 2. Fig. 2A shows the individual components that are needed for tight assembly of the cartridge. A detailed description of the material constituting the hollow fibers is available in the Methods section. Fig. 2B shows the assembly diagram of the hollow fibers, the acrylic covering and silicon gasket.

3.1. Morphological and functional properties of the NDIV-BBB

Visualization of intraluminally grown endothelial cells was achieved after fixation of individual capillaries as previously described [25,37,38,30,39]. To improve adhesion of endothelial cells to their substrate, we slightly modified the procedure used to inoculate the cells. Thus, instead of exposure of the cells to flow 2 h after seeding, we decided to 'bypass' the intraluminal perfusion pathway and expose the cells to abluminal flow (to grant oxygenation and nutrient delivery) for 1 day, prior to establishing intraluminal perfusion. While healthy growth of endothelial cells was achieved in both cases, we noted that multilayered piling of endothelial cells occurred in cells exposed to no flow for 24 h (compare Fig. 3A and 3C). When immediate exposure to flow was performed, monolayer growth and differentiation of endothelial cells was obtained, as previously described [25,37–39].

Visualization of abluminal glia was not possible when using the DIV-BBB. This limitation has been overcome with the new design, where positioning of the NDIV-BBB on a microscope stage is possible. Fig. 4D shows the appearance of living cells (C6) growing on the bottom of the apparatus, while Fig. 4E depicts the appearance of individual cells attached to the exterior of a hollow fiber.

Monitoring of cell metabolism is an essential step in assessing the quality of dynamically grown endothelial cells or glia [25,37,38,30]. Fig. 5A shows early changes in glucose consumption (open squares) lactate production (filled symbols) in bovine aortic endothelial cells grown in isolation or co-cultured with C6 glioma cells. Note the early peak in glucose consumption by BAEC shortly after culturing. The asterisks indicate statistically significant changes from previous measurement ($P<0.05$ by ANOVA). Addition of glial cells to the extraluminal compartment caused a robust increase in glucose consumption paralleled by analogous change in lactate production. In contrast to the prior design, the NDIV-BBB allows also for visualization of extracapillary growth (see below).

Parallel to metabolic changes, endothelial cells exposed to flow and glia developed functional specializations typical of blood–brain barrier endothelial cells (Fig. 5B). Thus, trans-endothelial electrical resistance increased dramatically after addition of glia to the abluminal compartment. BAEC alone developed a negligible increase in TEER during the time in culture. The resistance shown at $t=0$ is the background resistance of the NDIV-BBB apparatus.

3.2. Additional novel features in the NDIV-BBB

Biological events are characterized by a phenomenon-specific time course that helps unveil underlying mechanisms. Similarly, pathological events occur on widely different time scales, ranging from minutes to years. Unfortunately, many experimental conditions only allow for single time point evaluations. Thus, time-course investigations often require numerous parallel experiments. This was particularly true for the old dynamic model of the BBB, owing to its impenetrable nature and intrinsic design. To overcome this, a 'cranial window' was prearranged in the design of the NDIV-BBB (e.g. Figs. 2 and 3) to allow for sequential removal of individual capillaries while leaving the remaining ones intact. The morphological results presented in Fig. 4 were obtained on capillaries isolated during this procedure.

The viability of the remaining fibers was assessed by serial measurements of trans-endothelial resistance as shown in Fig. 6. Note that when the procedure was performed under sterile conditions and after suturing of the endings of the vessels that were removed, the TEER changed only slightly, demonstrating the functional survival of the remaining cells. A pictorial illustration of this procedure is shown in Fig. 6B.

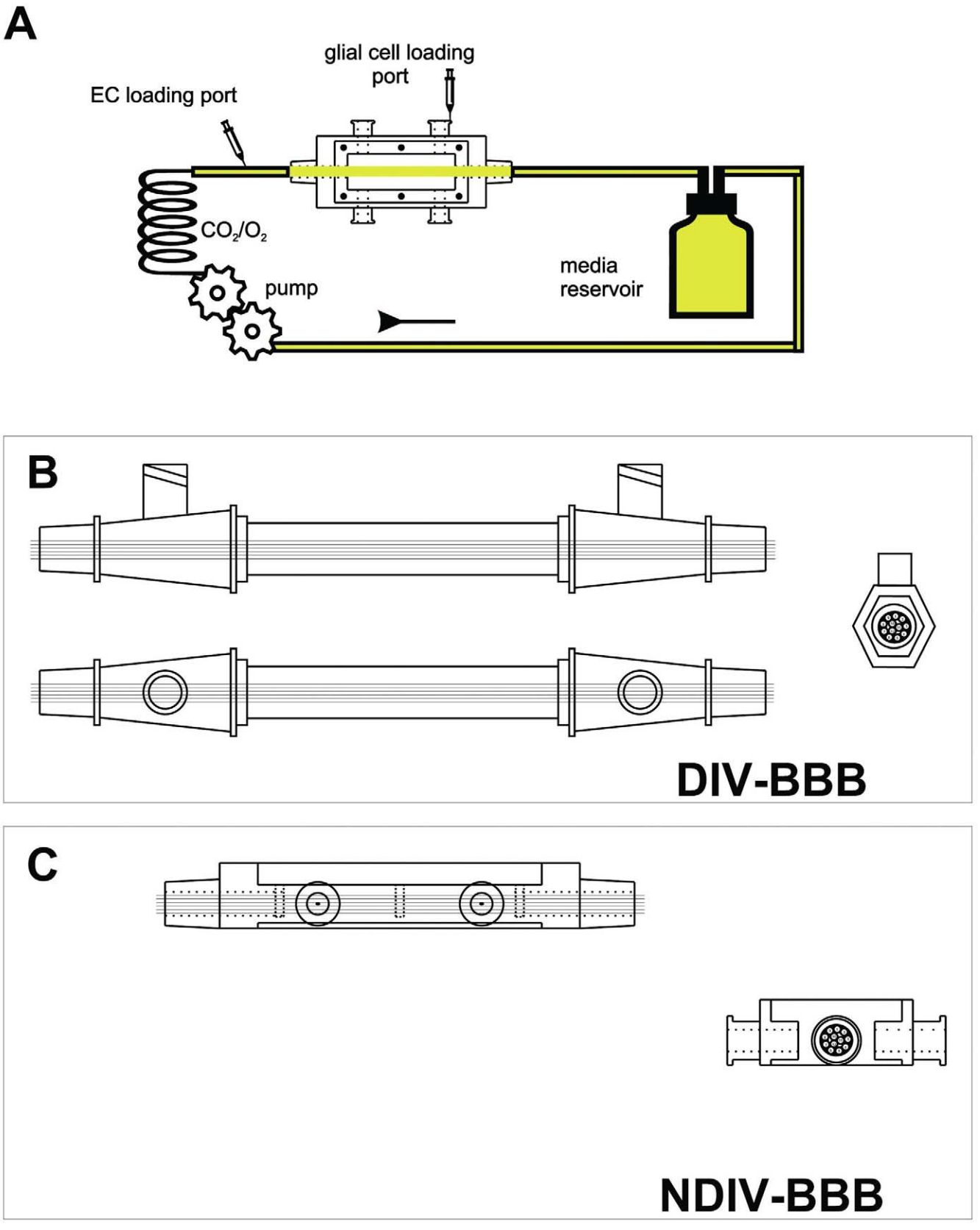

Fig. 1. Diagrammatic representation of the hollow fiber cartridge system and main differences between the DIV-BBB and the NDIV-BBB. A replaceable bundle of porous polypropylene hollow fibers is suspended in the chamber and is in continuity with a medium source through a flow path consisting of gas-permeable silicon tubing. A servo-controlled variable-speed pulsatile pump generates flow from the medium source through the capillary bundle and back. Note that (A) the assembly of the cartridge within a circulatory pathway to feed both endothelial and abluminally grown cells is identical for the two models. However, significant differences exist between the DIV-BBB and the NDIV-BBB as shown in longitudinal and cross-sections (B and C). See text for details.

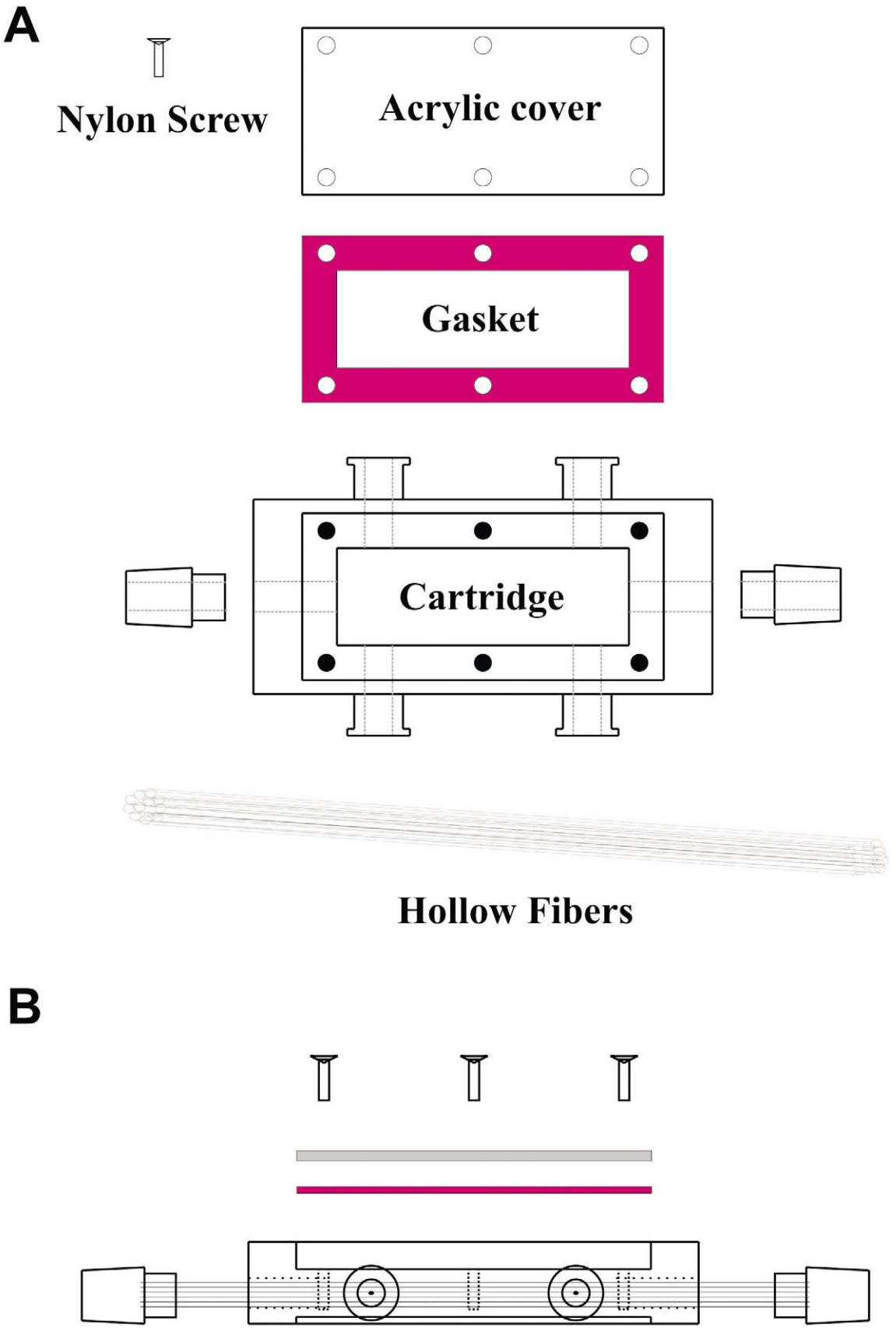

Fig. 2. Schematic representation of the assembly process of the NDIV-BBB. See text for details.

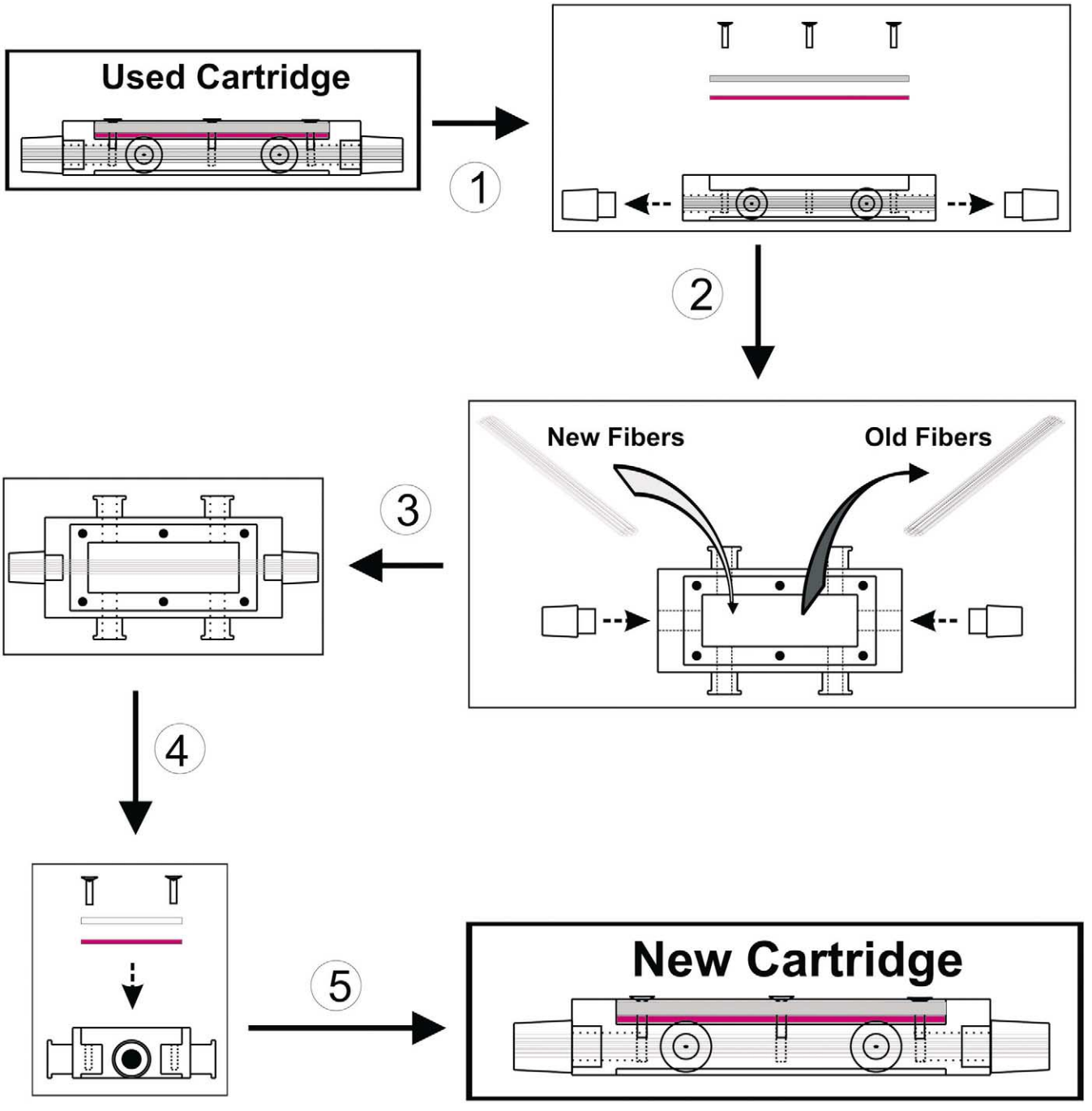

Fig. 3. Assembly properties and recyclable design of the NDIV-BBB.

3.3. Flow and pressure profiles in the NDIV-BBB

In previous papers, we and others have described the effects of flow on endothelial cell differentiation [17,16,7,15,6,8,20,26,42]. It is recognized, however, that different flow (shear) patterns influence endothelial cell physiology. We have thus investigated the profiles of pressure (pre- and post-hollow fibers) of the pulsatile flow provided by the QuadMax apparatus. The pulsation frequency used was 100 cycles per minute. Note (Fig. 7) that the flow pattern consisted of a complex waveform and that a substantial drop in pressure occurred at the end of the capillaries as expected in vivo. Details on this procedure and comparable experiments carried out on the DIV-BBB (old model) are available elsewhere [16,15].

4. Discussion

The main goal of the present study was to develop and

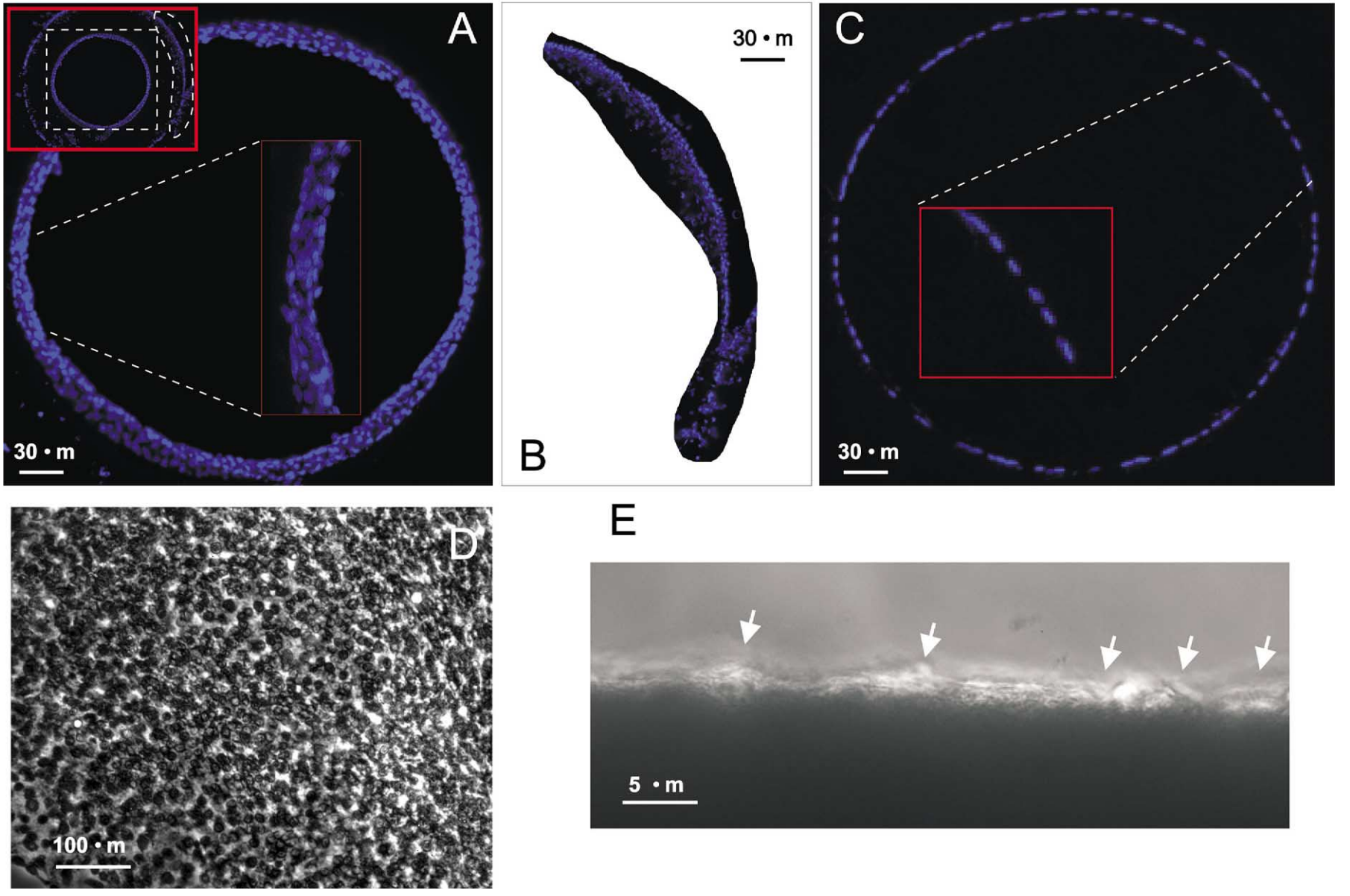

Fig. 4. Cellular growth patterns in hollow fibers. (A, C) Endothelial cells; (B) glia. Pictures were taken after 27 days in culture. Cells were stained with DAPI to visualize cell nuclei. This explains the gaps between blue stains. Note that endothelial cells grown initially under no flow conditions (A) tended to grow in a multilayered fashion. In contrast, early exposure to flow caused reduction of the cell number, and monolayer appearance of the endothelial cells (C). (B) Abluminal growth of C6 glioma cells. The insets in (A, C) show the portion of the hollow fibers from which pictures were taken. Sections had a thickness of 20 μm. (D) Appearance of glioma cells growing at the bottom of the NDIV-BBB. Growth of C6 glioma onto hollow fibers is shown in (E).

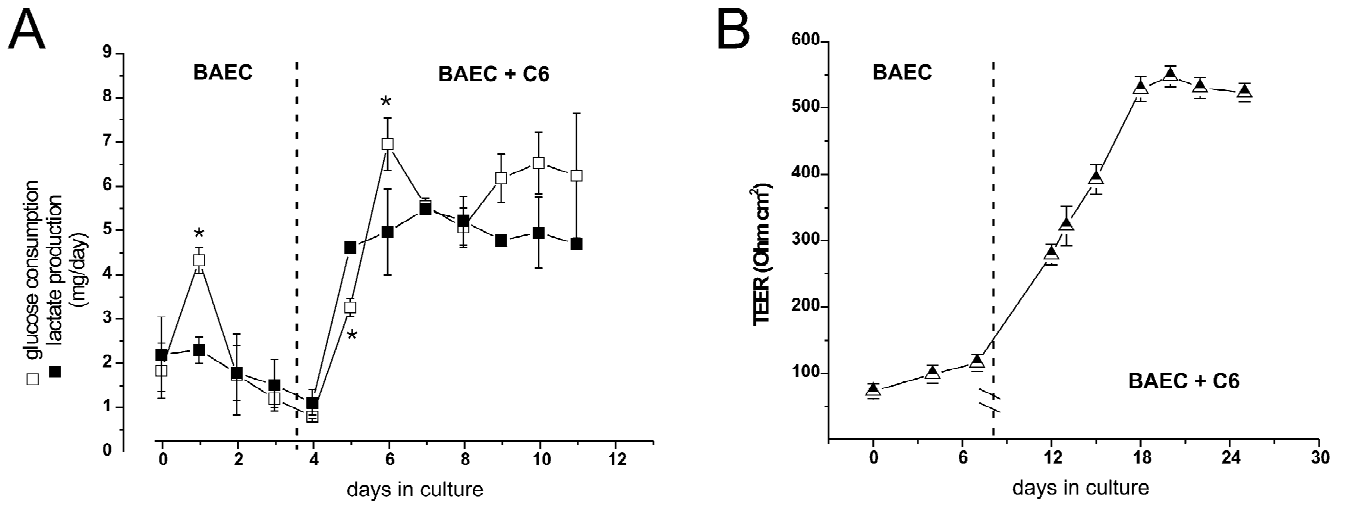

Fig. 5. Functional differentiation of hollow fiber-grown endothelial and C6 glioma cells. (A) Metabolism. Note the sharp increase in glucose consumption after 1 day of endothelial culturing. The asterisks refer to significant increase ($P<0.05$ by ANOVA) compared to previous value. Also note that the glucose consumption increased dramatically after addition of C6 cells. (B) TEER Trans-endothelial electrical resistance changes induced by co-culture of endothelial cells with glia.

characterize an in vitro model of the blood–brain barrier based on the recapitulation of the physiological properties of brain capillaries. To this end, and in an attempt to preserve the histological features of in situ microvessels, we have co-cultured endothelial cells and glia on a porous and permeable substrate aimed at mimicking the extracellular matrix. Endothelial cells were also exposed to physiologically relevant and amply modifiable flow patterns. Under these conditions, endothelial cells differentiated in a BBB-like phenotype. During this process, the model allowed experimentally timed excision of individual fibers that could then be processed for molecular, physiological, or morphological inspections. At the same time, growth of abluminal glia was monitored by conventional microscopic techniques.

Advances in molecular neurobiology are bringing us closer to the understanding of the etiology of chronic and acute degenerative brain disorders. A predictable result of the increased knowledge and awareness of CNS dysfunction mechanisms is the development of pharmaceutical strategies to treat a wide spectrum of neurological disorders. An equally foreseeable scenario is that most of the promising therapeutic approaches will fail the clinical challenge since most of the CNS drugs effective in vitro are effectively excluded by the blood–brain barrier [28,24]. Thus, it is imperative to develop a reliable model of the BBB that allows for inexpensive and mass testing of putative CNS therapeutic agents.

The use of cultured vascular endothelial cells as a model of vascular permeability has been well established and has yielded significant advancements in the understanding of microvascular physiology. However, serious limitations associated with the use of cultured brain endothelial cells have hampered the development of a reliable model of the blood–brain barrier. For example, it has been difficult to reproduce in cultured cells the high electrical resistance normally found across BBB endothelial cells in situ. Furthermore, cultured brain endothelial cells lose some of their specific markers following in vitro culturing [14]. One approach used to mimic the growth environment of in vivo brain EC has been the use of glia/endothelial co-cultures [4,5,1,3]. Alternatively, investigators have attempted to imitate the physiological environment of microvascular endothelial cells by exposing the cells to flow [7]. Stanness et al. combined these approaches [22,25,37,38,18,30,36,39].

Our present results confirm that dynamic modeling of the BBB is feasible and reproducible. In addition, we have exploited a number of additional properties of the system that may become useful for biomedical studies. In particular, we demonstrated that lack of exposure to flow promotes non-physiological cell cycle propensity in endothelial cells (e.g. Fig. 4). In fact, cells that were not constantly exposed to shear stress grew in multilayered fashion, while flow exposed cells did not. These morphological findings confirmed molecular data [17] as well as data from other laboratories [6,8,20,26,42] suggesting that cell cycle inhibition is an early event triggered by shear stress. This is an important finding, since it is known that brain microvessels are characterized by the presence of a single layer of endothelial cells. ‘Piling’ of cells may therefore be a feature of other non-flow based blood–brain barrier models, and may perhaps underlie TEER increases observed under conditions (EC alone) that do not cause TEER increases in the DIV-BBB.

Given the unquestionably relevance of preserved cerebral blood flow for EC functional maintenance, it was important to investigate the parameters of flow/shear stress in our model. Results obtained in the old DIV-BBB [16] suggested that the shape of the waveform and the pressure

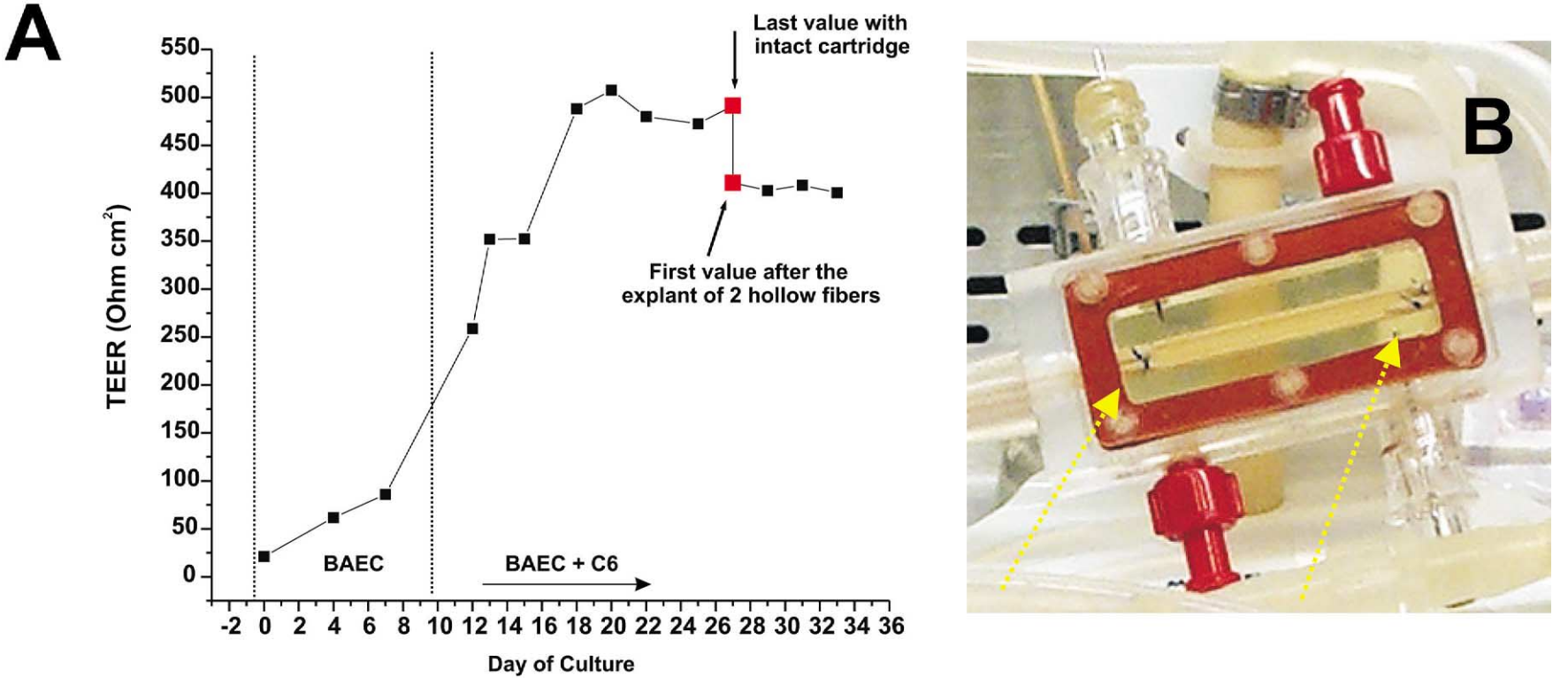

Fig. 6. Longitudinal studies of endothelial cell function in the NDIV-BBB. TEER was monitored as in Fig. 5B. After the system reached a stable TEER value of approximately 500 Ω cm^2, two individual capillaries were severed from the cartridge and removed under sterile conditions. The stubs were sutured with a polypropylene suture (Prolene). This is indicated in the picture to the right (arrows). Note that only slight TEER deterioration was observed after this procedure.

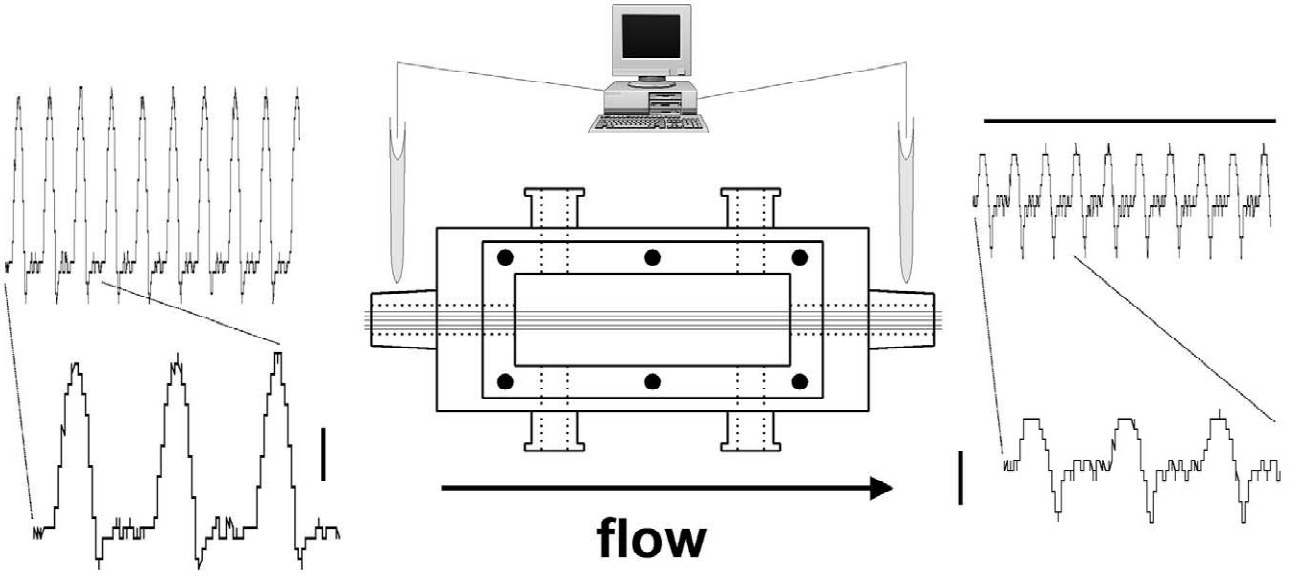

Fig. 7. Physiologically relevant pressure gradients between pre- and post-capillary segments recorded in the NDIV-BBB. Waveforms of pressure changes in pre- and post-capillary segments were concomitantly measured. Note that a significant drop in pressure occurred during passage through the capillaries and that the waveform was also significantly affected. The upper traces refer to measurements taken for 6 s, as indicated by the horizontal bar. Pulse frequency was 100 cycles per min. The vertical bar represents 5 mM Hg.

gradients were comparable to the in vivo flow. This was also the case in the NDIV-BBB where a significant drop from pre- to post-capillary pressure was observed. It is thus possible that the molecular, physiological and morphological results obtained in the (N)DIV-BBB are the summation of the properties of endothelial cells grown during exposure to physiologically relevant but variable levels of pressure/shear. This constitutes an advantage over rotation-based flow devices where uniform pressure accompanies shear gradients. However, it appears that flow, regardless of pressure, is a determinant of endothelial propensity towards cell division, since in both models shear inhibited division and expression of cell cycle related genes.

The fact that the NDIV-BBB allows excision of individual capillaries during culturing reveals a host of previously impractical or unfeasible cellular manipulations. For example, we have recently described the effects of flow cessation on EC properties by use of parallel experiments, i.e. where one cartridge served as a control to another [11]. In addition, each time point required 'sacrifice' of one DIV-BBB. By use of the NDIV-BBBB properties allowing serial observations over time, one may significantly decrease inter-experimental variability and thus greatly accelerate the discovery process. Similarly, dose–response, or time-course pharmacological experiments may also be carried out in individual cartridges. Finally, extraction of RNA/protein from individual fibers may allow to study how different cell-to-cell contacts (e.g. vascular smooth muscle vs. glia) may influence endothelial cell differentiation.

In conclusion, we have described the properties of a novel tissue culture apparatus that allows endothelial differentiation under controlled conditions that closely mimic the BBB in situ. Both flow and glia influenced endothelial cell differentiation. Future experiments will explore the possibility of using transparent hollow fibers to permit intravascular microscopy, as well as more complex designs including addition of blood and parenchymal cells (e.g. lymphocytes and microglia or vascular smooth muscle).

Acknowledgements

This work was supported by NIH-2RO1 HL51614, NIH-RO1 NINDS 43284 and NIH-RO1 NS38195 to DJ. LKB is supported by AHA-GIA.

References

[1] N.J. Abbott, P.A. Revest, Control of brain endothelial permeability, Cerebrovasc. Brain Metab. Rev. 3 (1991) 39–69.
[2] N.J. Abbott, I.A. Romero, Transporting therapeutics across the blood–brain barrier, Mol. Neurobiol. 2 (1994) 106–113.
[3] N.J. Abbott, P.A. Revest, I.A. Romero, Astrocyte–endothelial interaction: physiology and pathology, Neuropathol. Appl. Neurobiol. 18 (1992) 424–433.
[4] N.J. Abbott, F. Roux, P.O. Couraud, D.J. Begley, Studies on an immortalized brain endothelial cell line: differentiation, permeability and transport, in: J. Greenwood, D.J. Begley, M.B. Segal (Eds.), Current Concepts of a Blood–Brain Barrier, Plenum, New York, 1995, pp. 239–249.
[5] N.J. Abbott, C.C. Hughes, P.A. Revest, J. Greenwood, Development and characterisation of a rat brain capillary endothelial culture:

towards an in vitro blood–brain barrier, J. Cell Sci. 103 (1992) 23–37.
[6] S. Akimoto, M. Mitsumata, T. Sasaguri, Y. Yoshida, Laminar shear stress inhibits vascular endothelial cell proliferation by inducing cyclin-dependent kinase inhibitor p21$^{Sdil/Cip1/Waf1}$, Circ. Res. 86 (2000) 185–190.
[7] B.J. Ballermann, A. Dardik, E. Eng, A. Liu, Shear stress and the endothelium, Kidney Int. Suppl. 67 (1998) S100–S108.
[8] X. Bao, C. Lu, J.A. Frangos, Temporal gradient in shear but not steady shear stress induces PDGF-A and MCP-1 expression in endothelial cells: role of NO, NF kappa B, and egr-1, Arterioscler. Thromb. Vasc. Biol. 19 (1999) 996–1003.
[9] X. Bao, C.B. Clark, J.A. Frangos, Temporal gradient in shear-induced signaling pathway: involvement of MAP kinase, c-fos, and connexin43, Am. J. Physiol. Heart Circ. Physiol. 278 (2000) H1598–H1605.
[10] D.J. Begley, D. Lechardeur, Z.D. Chen, C. Rollinson, M. Bardoul, F. Roux, D. Scherman, N.J. Abbott, Functional expression of P-glycoprotein in an immortalised cell line of rat brain endothelial cells, RBE4, J. Neurochem. 67 (1996) 988–995.
[11] L. Bengez, M. Kapural, F.E. Parkinson, M. Hossein, A. Barth, D. Janigro, The role of flow cessation on endothelial-glia communication at the blood–brain barrier. Soc. Neurosci. Abstr., 27 (2001).
[12] A.L. Betz, Transport of ions across the blood–brain barrier, Fed. Proc. 45 (1986) 2050–2054.
[13] L. Cucullo, M. Marroni, G.A. Grant, M. Kinter, S. Desai, M.R. Mayberg, K. Signorelli, D. Janigro, Genomics and proteomics of the human blood–brain barrier. Soc. Neurosci. Abstr., 27 (2001).
[14] L.E. De Bault, P.A. Cancilla, Gammaglutamyl transpeptidase in isolated brain endothelial cells: induction by glial cells in vitro, Science 207 (1980) 653–655.
[15] S. Desai, M.R. Mayberg, L. Bengez, D. Janigro, The DIV-BBB: A powerful tool to study gene expression changes in endothelial cells, Endothelium 7 (2001) 201.
[16] S. Desai, M. Marroni, L. Cucullo, L. Bengez, M. Hossein, M.R. Mayberg, G.A. Grant, D. Janigro, Mechanisms of endothelial survival under shear stress, Endothelium 9 (2002) 89–102.
[17] S. Desai, M.S. McAllister, M.R. Mayberg, D. Janigro, Mechanisms of endothelial survival under shear stress, in: D. Kobiler, H.S. Lustig, S. Shapira (Eds.), Blood–Brain Barrier Delivery and Brain Pathology, Kluwer, Dordrecht, 2001, pp. 63–70.
[18] G.A. Grant, N.J. Abbott, D. Janigro, Understanding the physiology of the blood–brain barrier: in vitro models, News Physiol. Sci. 13 (1998) 287–293.
[19] M.A. Haidekker, N. L'Heureux, J.A. Frangos, Fluid shear stress increases membrane fluidity in endothelial cells: a study with DCVJ fluorescence, Am. J. Physiol. Heart Circ. Physiol. 278 (2000) H1401–H1406.
[20] B.W. Hochleitner, E.O. Hochleitner, P. Obrist, T. Eberl, A. Amberger, Q. Xu, R. Margreiter, G. Wick, Fluid shear stress induces heat shock protein 60 expression in endothelial cells in vitro and in vivo, Arterioscler. Thromb. Vasc. Biol. 20 (2000) 617–623.
[21] D. Janigro, K.A. Stanness, C. Soderland, A.G. Grant, Development of an in vitro blood–brain barrier. In: Biochemical and Molecular Neurotoxicology, Wiley, New York, 2000, pp. 12.2.1–12.2.10.
[22] D. Janigro, S.M. Leaman, K.A. Stanness, Dynamic modeling of the blood–brain barrier: a novel tool for studies of drug delivery to the brain, Pharm. Sci. Technol. Today 2 (1999) 7–12.
[23] D. Janigro, K.A. Stanness, T.-S. Nguyen, D.L. Tinklepaugh, H.R. Winn, Possible role of glia in the induction of CNS-like properties in aortic endothelial cells: ATP-activated channels, in: L. Bellardinelli, A. Pelleg (Eds.), Adenosine and Adenine Nucleotides, Nijhoff, Boston, 1996, pp. 85–96.
[24] S. Kim, S. Scheerer, M.A. Geyer, S.B. Howell, Direct cerebrospinal fluid delivery of an antiretroviral agent using multivesicular liposomes, J. Infect. Dis. 162 (1990) 750–752.
[25] M.S. McAllister, L. Krizanac-Bengez, F. Macchia, R.J. Naftalin, K.C. Pedley, M.R. Mayberg, M. Marroni, S. Leaman, K.A. Stanness, D. Janigro, Mechanisms of glucose transport at the blood–brain barrier: an in vitro study, Brain Res. 904 (2001) 20–30.
[26] T. Nagel, N. Resnick, W.J. Atkinson, C.F. Dewey, M.A. Gimbrone, Shear stress selectively upregulates intercellular adhesion molecule-1 expression in cultured human vascular endothelial cells, J. Clin. Invest. 94 (1994) 885–891.
[27] M.J. Ott, J.L. Olson, B.J. Ballermann, Chronic *in vitro* flow promotes ultrastructural differentiation of endothelial cells, Endothelium 3 (1995) 21–30.
[28] W.M. Pardridge, Why is the global CNS pharmaceutical market so under-penetrated?, Drug Discov. Today 7 (2002) 5–7.
[29] F.E. Parkinson, A.R.P. Paterson, J.D. Young, C.E. Cass, Inhibitory effects of propentofylline on adenosine influx, Biochem. Pharmacol. 46 (1993) 891–896.
[30] M. Pekny, K.A. Stanness, C. Eliasson, C. Betsholtz, D. Janigro, Impaired induction of blood–brain barrier properties in aortic endothelial cells by astrocytes from GFAP-deficient mice, Glia 22 (1998) 390–400.
[31] T.H. Pohlman, J.M. Harlan, Adaptive responses of the endothelium to stress, J. Surg. Res. 89 (2000) 85–119.
[32] W. Risau, S. Esser, B. Engelhardt, Differentiation of blood–brain barrier endothelial cells, Pathol. Biol. Paris 46 (1998) 171–175.
[33] L.L. Rubin, J.M. Staddon, The cell biology of the blood–brain barrier, Annu. Rev. Neurosci. 22 (1999) 11–28.
[34] F. Salvetti, F. Ceci, D. Janigro, A. Lucacchini, L. Benzi, C. Martini, Insulin permeability across an in vitro model of the endothelium, Pharm. Res. 19 (2002) 445–450.
[35] A.H. Schinkel, P-Glycoprotein, a gatekeeper in the blood–brain barrier, Adv. Drug Deliv. Rev. 36 (1999) 179–194.
[36] C.J. Sinclair, L. Krizanac-Bengez, K.A. Stanness, D. Janigro, F.E. Parkinson, Adenosine permeation of a dynamic in vitro blood–brain barrier inhibited by dipyridamole, Brain Res. 898 (2001) 122–125.
[37] K.A. Stanness, E. Guatteo, D. Janigro, A dynamic model of the blood–brain barrier 'in vitro', Neurotoxicology 17 (1996) 481–496.
[38] K.A. Stanness, L.E. Westrum, E. Fornaciari, P. Mascagni, J.A. Nelson, S.G. Stenglein, T. Myers, D. Janigro, Morphological and functional characterization of an in vitro blood–brain barrier model, Brain Res. 771 (1997) 329–342.
[39] K.A. Stanness, J.F. Neumaier, T.J. Sexton, G.A. Grant, A. Emmi, D.O. Maris, D. Janigro, A new model of the blood–brain barrier: co-culture of neuronal, endothelial and glial cells under dynamic conditions, Neuroreport 10 (1999) 3725–3731.
[40] L. Strelow, D. Janigro, J.A. Nelson, The blood–brain barrier and AIDS, Adv. Virus Res. 56 (2001) 355–388.
[41] H. Tsukamoto, Y. Hamada, D. Wu, R.J. Boado, W.M. Pardridge, GLUT1 glucose transporter: differential gene transcription and mRNA binding to cytosolic and polysome proteins in brain and peripheral tissues, Brain Res. Mol. Brain Res. 58 (1998) 170–177.
[42] S. Zhao, A. Suciu, T. Ziegler, J.E. Moore Jr., E. Burki, J.J. Meister, H.R. Brunner, Synergistic effects of fluid shear stress and cyclic circumferential stretch on vascular endothelial cell morphology and cytoskeleton, Arterioscler. Thromb. Vasc. Biol. 15 (1995) 1781–1786.